Evidence for a Metal−Thiolate Intermediate in Alkyl Group Transfer from Epoxypropane to Coenzyme M and Cooperative Metal Ion Binding in Epoxyalkane:CoM Transferase†

Jeffrey M. Boyd and Scott A. Ensign*

Department of Chemistry and Biochemistry, Utah State University, Logan, Utah 84322

Received March 28, 2005; Revised Manuscript Received August 4, 2005

ABSTRACT: Epoxyalkane:coenzyme M transferase (EaCoMT) catalyzes the nucleophilic addition of coenzyme M (CoM, 2-mercaptoethanesulfonic acid) to epoxypropane forming 2-hydroxypropyl-CoM. The biochemical properties of EaCoMT suggest that the enzyme belongs to the family of alkyltransferase enzymes for which Zn plays a role in activating an organic thiol substrate for nucleophilic attack on an alkyl-donating substrate. The enzyme has a hexameric (α_6) structure with one zinc atom per subunit. In the present work M^{2+} binding and the role of Zn^{2+} in EaCoMT have been established through a combination of biochemical, calorimetric, and spectroscopic techniques. A variety of metal ions, including Zn^{2+}, Co^{2+}, Cd^{2+}, and Ni^{2+}, were capable of activating a Zn-deficient "apo" form of EaCoMT, affording enzymes with various levels of activity. Titration of Co^{2+} into apo-EaCoMT resulted in UV−visible spectroscopic changes consistent with the formation of a tetrahedral Co^{2+} binding site, with coordination of bound Co^{2+} to two thiolate ligands. Quantification of UV−visible spectral changes upon Co^{2+} titration into apo-EaCoMT demonstrated that EaCoMT binds Co^{2+} cooperatively at six interacting sites. Isothermal titration calorimetric studies of Co^{2+} and Zn^{2+} binding to EaCoMT also showed cooperativity for metal ion binding among six sites. The addition of CoM to Co^{2+}-substituted EaCoMT resulted in UV−visible spectral changes indicative of formation of a new thiol−Co^{2+} bond. Co^{2+}-substituted EaCoMT exhibited a unique Co^{2+} EPR spectrum, and this spectrum was perturbed significantly upon addition of CoM. The presence of a divalent metal ion was required for the release of protons from CoM upon binding to EaCoMT, with Zn^{2+}, Co^{2+}, and Cd^{2+} each facilitating proton release. The divalent metal ion of EaCoMT is proposed to play a key role in the coordination and deprotonation of CoM, possibly through formation of a metal−thiolate that is activated for attack on the epoxide substrate.

The microbial metabolism of short-chain aliphatic alkenes such as ethylene and propylene is initiated by the monooxygenase-catalyzed insertion of an oxygen atom into the olefin bond to form the corresponding epoxide, as shown in the equation (*1*, *2*):

$$\text{propylene} + \text{NADH} + \text{H}^+ + \text{O}_2 \xrightarrow{\text{alkene monooxygenase}} \text{epoxypropane} + \text{NAD}^+ + \text{H}_2\text{O} \quad (1)$$

Epoxides thus formed are further metabolized by a sequence of reactions that uses the atypical cofactor coenzyme M (2-mercaptoethanesulfonic acid, CoM)[1] as a nucleophile for epoxide ring opening and as the carrier of activated intermediates that undergo further enzymatic transformations, ultimately resulting in conversion to central metabolites (*3*−*5*). The nucleophilic attack of CoM on the epoxide is catalyzed by epoxyalkane:CoM transferase (EaCoMT), which forms a hydroxyalkyl thioether conjugate of the epoxide and CoM as shown in the equation (*4*):

$$\text{HS-CoM} + \text{epoxypropane} \xrightarrow{\text{epoxyalkane:CoM transferase (EaCoMT)}} \text{2-hydroxypropyl-CoM} \quad (2)$$

Nucleophilic addition to CoM represents the most recently discovered enzyme-catalyzed transformation of aliphatic epoxides and the only known reaction whereby short-chain aliphatic epoxides formed from monounsaturated alkene oxidation are productively metabolized as carbon and energy sources to support microbial growth (*4*−*6*).

† This work was supported by National Institutes of Health Grant GM51805.

* Corresponding author: (435) 797-3969 (phone); (435) 797-3390 (fax); ensigns@cc.usu.edu (e-mail).

[1] Abbreviations: CDTA, *trans*-1,2-diaminocyclohexane-*N*,*N*,*N*′,*N*′-tetraacetic acid; CoM, coenzyme M (2-mercaptoethanesulfonic acid); EaCoMT, epoxyalkane:CoM transferase [EC 4.2.99.19; systematic name, 2-hydroxypropyl-CoM:2-mercaptoethanesulfonate lyase (epoxyalkane-ring-forming)]; EPR, electron paramagnetic resonance; EXAFS, extended X-ray absorption fine structure; ICP-MS, inductively coupled plasma atomic emission mass spectrometry; ITC, isothermal titration calorimetry; LMCT, ligand to metal charge transfer; MetE, cobalamin-independent methionine synthase; MOPS, 3-(*N*-morpholino)propanesulfonic acid; MT2-A, methylcobamide:CoM methyltransferase 2-A (MtbA); MT2-M, methylcobamide:CoM methyltransferase 2-M (MtaA); PAR, 4-(2-pyridylazo)resorcinol; PMPS, *p*-(hydroxymercuri)benzenesulfonic acid; TCEP, tris(2-carboxyethyl)phosphine hydrochloride; THF, tetrahydrofolate.

10.1021/bi0505619 CCC: $30.25
Published on Web 09/10/2005

The biochemical, molecular, and genetic characterization of EaCoMT reveals that it belongs to the family of zinc-dependent enzymes that catalyze alkyl group transfer to an organic thiol (*7*). Other enzymes within this broad family include cobalamin-dependent methionine synthase (MetH) (*8*), cobalamin-independent methionine synthase (MetE) (*9*), the Ada protein (*10*), protein farnesyl transferase (*11*), human betaine−homocysteine methyltransferase (*12*), *S*-methylmethionine:homocysteine methyltransferase (*13*), and methylcobamide:CoM methyltransferases (MT2-A and MT2-M) (*14*, *15*). Among these zinc alkyltransferases, a subset of enzymes, which includes MetE, EaCoMT, MT2-A, and MT2-M, contains a characteristic Cys-X-His-X_n-Cys motif first identified in MetE (*9*, *14*−*16*). Biochemical (*9*, *17*), spectroscopic (*9*, *18*), and structural (*19*, *20*) studies of MetE have shown that these three amino acids are ligands to the Zn^{2+} center, while an exogenous water molecule (*19*) or glutamate residue (*20*) is believed to serve as the fourth ligand. EXAFS studies have provided evidence that coordination of the substrate homocysteine to the zinc center lowers the pK_a of homocysteine, activating it for nucleophilic attack on the second substrate methyl-THF (*21*). Biochemical and spectroscopic studies of MT2-A, MT2-M, and EaCoMT have led to similar proposals for activation of CoM by coordination to the Zn^{2+} center (*7*, *14*, *15*, *22*). Recent crystallographic studies of MetE from two organisms suggest that homocysteine may not bind directly to the zinc center but instead that a ligand rearrangement at the Zn^{2+} center occurs upon homocysteine binding, resulting in substantial changes in the geometry and coordination number about Zn^{2+} (*19*, *20*).

A number of features of EaCoMT distinguish it from all other zinc alkyltransferases, most notably the nature of the reaction itself. All other members of this family catalyze the nucleophilic displacement of an alkyl group from a donor molecule to the thiol acceptor, resulting in a dealkylated donor and alkylated thiol. In contrast, the reaction catalyzed by EaCoMT is a nucleophilic addition reaction, as shown in eq 2. Another distinguishing feature of EaCoMT relates to its subunit composition, which is a hexameric unit of identical subunits. In contrast, all other enzymes containing the MetE-like Zn^{2+} binding motif are monomers, with the exception of methylthiol:CoM methyltransferase from *Methanosarcina barkeri*, which is also a multimer (*23*). As a final distinguishing feature, EaCoMT is the only known enzyme outside of the archaeal kingdom that uses free CoM as a substrate/cofactor (*4*). Prior to the identification of CoM in bacterial alkene metabolism, the only known function for this cofactor was in archaeal methanogenesis (*24*−*26*).

Previous studies of Zn-containing and Zn-depleted wild-type and site-directed mutants of EaCoMT have shown that Zn is required for enzymatic activity (*7*). Additionally, calorimetric studies revealed that CoM binds stoichiometrically and with high affinity ($K_d = 3.8\ \mu M$) to Zn-containing EaCoMT but not to the Zn-deficient enzyme (*7*). Calorimetric studies of the binding of CoM analogues to EaCoMT also allowed the thermodynamic contributions of the thiol, alkyl, and sulfonate groups to binding of CoM to be determined (*7*). A kinetic analysis of the pH dependence of the reaction indicated that binding of CoM to EaCoMT results in a lowering of the pK_a of CoM from 9.1 to 7.4, presumably via stabilization of the CoM thiolate by binding to the Zn^{2+} center (*7*).

While the previous studies of EaCoMT support a role for Zn^{2+} in CoM binding and activation, this interaction has not been demonstrated directly by spectroscopic techniques. The paramagnetic properties of Co^{2+}, and its ability to substitute for Zn^{2+} in many metalloenzymes, make it an excellent probe for studying biological Zn^{2+} centers (*27*, *28*), including those within the alkyltransferase family (*14*, *29*, *30*). Accordingly, in the present study, the binding and association of Co^{2+} with Zn-deficient "apo"-EaCoMT, and the subsequent binding of CoM to the Co^{2+}-substituted enzyme, have been investigated using UV−visible and EPR spectrotrometry. These studies support the proposal that ligand rearrangement occurs upon binding of CoM to EaCoMT, with evidence for the formation of a new metal−thiolate bond. Additionally, calorimetric studies of Co^{2+} and Zn^{2+} binding to apo-EaCoMT, together with UV−visible spectroscopic studies of Co^{2+} binding, demonstrate that the binding of metal ions to EaCoMT occurs in a cooperative fashion. Finally, the role of Zn^{2+} in CoM thiol deprotonation is demonstrated directly by proton release studies with the apoenzyme and Zn^{2+}-, Co^{2+}-, and Cd^{2+}-bound enzymes.

EXPERIMENTAL PROCEDURES

Materials. Racemic propylene oxide (>99%), 2-mercaptoethanesulfonic acid (coenzyme M), 4-(2-pyridylazo)resorcinol (PAR), and *p*-(hydroxymercuri)benzenesulfonic acid (PMPS) were purchased from Sigma-Aldrich Chemical Co. Tris(2-carboxyethyl)phosphine hydrochloride (TCEP) was purchased from Pierce. Cobalt chloride, ACS grade, was purchased from Fisher. All other chemicals used were of the highest purity available.

Buffer Preparation and Anaerobic Work. All solutions were prepared using deionized water (Barnstead) treated with Chelex-100 resin (Bio-Rad). Buffer A, 50 mM Tris-HCl, pH 8.0, with 10% glycerol (v/v), was run over a column of Chelex resin before use. All glassware was washed in 1 M HNO_3.

Anaerobic work was performed using a Vacuum Atmospheres Co. anaerobic glovebox or vacuum manifold. Before placement inside the anaerobic chamber, solutions were made anoxic by repeated evacuation and flushing with N_2 or Ar gas passed over columns of heated Cu and ascarite II for removal of O_2 and CO_2, respectively. Outside of the glovebox all solutions were added to samples using gastight Hamilton syringes. Unless indicated otherwise, all incubations and manipulations were performed under anaerobic conditions.

Protein Expression and Purification. As previously described, EaCoMT was expressed in *Escherichia coli* strain BL21(DE3) grown at 37 °C in the presence of 1 mM EDTA to prevent free zinc binding to EaCoMT (*7*). EaCoMT was purified as described previously using buffer which had 1 mM EDTA and 2 mM DTT added after Chelex treatment (*7*). When the enzyme was shown to be ≥95% pure by SDS−PAGE analysis, fractions containing EaCoMT were combined and concentrated over a 30000 MW cutoff membrane (Amicon YM30) to ≥80 mg·mL^{-1}. After concentration, the enzyme was dialyzed overnight in 50 mM Tris-HCl, pH 7.3, 10% (v/v) glycerol, and 5 mM CDTA. CDTA was then removed from the enzyme solution by a

6 h dialysis against buffer A containing 2 mM DTT and free Chelex resin. The purified protein, free from metal chelators, was concentrated, pelleted into liquid nitrogen, and stored at −80 °C until needed. All steps were performed at 4 °C, and buffers used for dialysis had the pH adjusted at 4 °C.

Gas Chromatographic Assay of EaCoMT Activity. Assays (1 mL total volume) were performed at 30 °C in anaerobically prepared serum vials (9 mL) which contained enzyme (70 nM purified protein from a 35 μM stock solution), 5 mM CoM, 4 mM freshly prepared propylene oxide, metal salt (0−60 μM), and buffer A. Coenzyme M and propylene oxide were prepared as 500 mM stock solutions in water. For assays in which metal was added, enzyme, buffer, and metal were incubated on ice in serum vials for 15 min prior to CoM addition. All assays were initiated by the addition of 4 mM propylene oxide. Samples were incubated at 30 °C in a shaking water bath at 200 cycles/min. At desired time points, using a gastight Hamilton syringe, 100 μL samples were removed from the headspace of the assay vials, and the amount of epoxypropane remaining was determined by gas chromatography(*4*).

UV−Visible Spectroscopic Titration of Apo-EaCoMT with Co^{2+}. Cobalt ion association with EaCoMT was monitored spectrophotometrically using a Shimadzu UV-2401PC UV−visible spectrophotometer interfaced to a PC with Shimadzu Spectroscopy Software Revision 3.7. Before sample preparation a baseline was run with 200 μL of buffer A in an acid-washed 250 μL quartz cuvette. Two hundred microliters of apo-EaCoMT/buffer A, with a concentration of 358 μM (71.6 nmol), was placed in the 250 μL quartz cuvette sealed with a 10 × 20 mm white rubber stopper. TCEP, from a 100 mM stock solution prepared in water, was then added to the cuvette to a concentration of 1 mM. A spectrum of the apo-EaCoMT was recorded which could be subtracted from subsequent spectra of EaCoMT in which Co^{2+} had been titrated. Spectra were recorded after each 2 μL (20 nmol) addition of $CoCl_2$ from a 10 mM stock prepared anoxically in buffer A. After each titrant addition the sample was incubated for 3−5 min at room temperature before the spectrum was recorded. For spectral comparison, 10 mM $CoCl_2$ prepared in buffer A was titrated into buffer A containing 1 mM TCEP. Using SigmaPlot 8.0, spectra of the $CoCl_2$ titrations were corrected for dilution by multiplication by a dilution factor before data analysis. All spectra were recorded at 23 °C.

UV−Visible Spectroscopy of Co^{2+}-Substituted EaCoMT Titrated with Coenzyme M. EaCoMT, diluted in buffer A, was placed in a 9 mL serum vial inside the glovebox. The sample was then reduced with 1 mM TCEP taken from a 100 mM stock solution prepared in water. Cobalt chloride was added in a 2.5-fold ($M_{Co}/M_{metal\ site}$) excess from a 100 mM stock solution prepared in water, and the sample was incubated for 30 min at room temperature. The Co^{2+}-loaded sample was then run over a PD-10 size exclusion column (Amersham Pharmacia Biotech AB) which had 1.5 cm of Chelex resin placed atop the factory-placed plastic frit. The Co^{2+}-loaded protein was concentrated by centrifugation using a 2 mL Centricon YM-100 (Amicon) placed within a sealed 40 mL centrifuge tube containing an N_2 atmosphere. The sample was pelleted into liquid N_2 and stored at −80 °C until needed. A baseline was established with buffer A using a 250 μL quartz cuvette which was sealed with an acid-washed white 10 × 20 mm rubber stopper. Two hundred microliters of the blue enzyme (304 μM) was added to the empty cuvette followed by the addition of TCEP to a concentration of 1 mM. A spectrum of Co^{2+}-loaded EaCoMT was recorded, and subsequent spectra were recorded after 2 μL additions of CoM from a 5 mM stock prepared in buffer A. After each addition of CoM the samples were allowed to incubate for 3−5 min before spectra were recorded. Each spectrum was corrected for dilution before binding analysis using SigmaPlot 8.0. All spectra were recorded at 23 °C.

Isothermal Titration Calorimetry. Isothermal titration calorimetry was performed using a MicroCal titration microcalorimeter (Northampton, MA). Metal solutions were prepared in buffer A which was previously used for overnight enzyme dialysis at 4 °C. This ensured that the protein buffer and the buffer used for metal preparation were identical, which decreases background heat which can be seen from buffer dilution. All solutions were vigorously degassed prior to use. For all reactions the reference offset was 30%, and the reaction temperature was 30 °C with a syringe stirring speed of 150 rpm. The reaction and reference cells had a volume of 1.374 mL. The protein concentration was 10 μM. Metal (1−5 mM) was also titrated into buffer to determine the heat of dilution. Background heats were subtracted from data before the thermograms were evaluated. Thermogram data were analyzed using the ORIGIN software supplied by MicroCal Inc. Thermodynamic parameters are presented in accordance with the recent recommendations of biochemical thermodynamic data (*31*).

EPR Spectroscopy of Cobalt-Substituted EaCoMT. X-band EPR spectra were obtained using a Bruker model ESP 300 spectrometer equipped with an ER 4116 DM dual mode X-band cavity and an Oxford Instruments ESR-900 helium flow cryostat. In all cases, calibrated 4 mm quartz EPR tubes (Wilmad, Buena, NJ) were used. Independently recorded background spectra of the cavity were aligned with and subtracted from experimental spectra. EPR spectra were recorded at a modulation frequency of 100 kHz and a modulation amplitude of 1.26 mT (12.6 G), with a sweep rate of 10 mT s^{-1}. Spectra were recorded at microwave frequencies of approximately 9.64 GHz, with the precise microwave frequencies noted for individual spectra to ensure exact *g*-alignment.

Co^{2+}-loaded EaCoMT used for EPR analysis was prepared as described above. For EPR analyses of purified protein, samples were diluted with buffer A to a concentration of 238 μM. CoM was added from a 500 mM stock solution. The EPR tubes had a total volume of 300 μL protein plus substrates. Spectra shown are the average of six scans.

Proton Release Assay. Proton release upon CoM titration into metal-substituted EaCoMT was determined by the method described by Goulding and Matthews for cobalamin-dependent methionine synthase (*8*). Apo-EaCoMT samples (90 mg·mL^{-1} protein/buffer A stock) were diluted to 1.5 mL with 50 μM Tris-HCl, pH 7.8, 10% glycerol (vol/vol), 50 mM NaCl, and 40 μM phenol red (buffer B) to reach an approximate protein concentration of 40 mg·mL^{-1}. Metal salts ($ZnCl_2$, $CoCl_2$, or $CdCl_2$) were then added to a final concentration of 2.15 mM (∼2.15 excess $M_{metal}/M_{metal\ site}$) in three of the samples, and one sample was left in the apo form. These solutions were allowed to incubate on ice for

2 h before the protein samples were run over Chelex-100 and PD-10 size exclusion columns (see above) equilibrated with buffer B. The samples were individually dialyzed overnight against 5 L of buffer B at 4 °C. Coenzyme M, the titrant, was prepared as a 1 mM stock in buffer B. This solution was continually bubbled with nitrogen gas to remove all dissolved O_2 and CO_2 from the reaction mixture. The modified glassware used to remove O_2 and CO_2 from the CoM solution had a side port in which a pH electrode (Accument basic AB15 Fisher Scientific) was placed, and the pH of the solution was continually monitored. The pH of the solution was maintained at 7.8 by the addition of either 10 mM NaOH or HCl. EaCoMT samples were diluted with buffer B to concentrations of 30 μM, and 1 mL samples were placed in a modified quartz cuvette with a crimp seal top and sealed with a butyl rubber stopper under an atmosphere of N_2. Two microliter additions of a CoM stock solution, prepared in buffer B, were then made to the protein solution. The change in A_{558} was recorded after each CoM addition once the absorbance was stable (approximately 1 min). The change in absorbance per mole of protons released into solution was determined by titrating the solution of buffer B with 1 mM HCl and monitoring the change in A_{558}. For all proton release assays a UV160U Shimatzu UV−visible spectrophotometer was used.

Analytical Procedures. Protein concentrations were determined by means of a modified biuret assay using bovine serum albumin as a standard (*32*). Metal analysis were performed by ICP-MS at the Utah State University Veterinary Diagnostics Laboratory and by the PAR/PMPS assay modified by Krum et al. (*7*, *9*). Before samples were analyzed by metal analysis, they were desalted and/or chelexed to remove any adventitiously bound metal. Densitometric analysis of bands in SDS−PAGE gels was performed using a FujiFilm model LAS-3000 image reader with Luminescent Image Analyzer photosoftware.

RESULTS

Preparation of Zn-Deficient EaCoMT and Activation by Divalent Metal Ions. In a previous study, the requirement of Zn^{2+} for EaCoMT activity was established in two ways: by removing Zn^{2+} from the holoenzyme using the reagents PAR and PMPS and by expressing EaCoMT in media containing EDTA and subsequently purifying the enzyme to homogeneity in buffers containing EDTA (*7*). The former treatment resulted in the stoichiometric removal of Zn^{2+} from EaCoMT with concomitant loss of catalytic activity, but the Zn-deficient enzyme thus formed could not be fully activated by adding Zn^{2+} back, presumably due to damage incurred by the harsh PMPS/PAR treatment (*7*). The latter procedure (expression and purification in the presence of EDTA) afforded a Zn-deficient enzyme that contained approximately 0.2 mol of Zn/mol of active site, and with a specific activity that was ~25% of the holoenzyme, showing a direct correlation between Zn content and specific activity (*7*). Expression and purification in the presence of EDTA were not sufficient, however, to obtain an enzyme preparation completely devoid of Zn.

In the present study, we investigated the conditions necessary for preparation of a quantitatively Zn^{2+}-deficient form of EaCoMT that could be activated by addition of exogenous Zn^{2+}. Incubation of holo-EaCoMT with EDTA or EGTA resulted in little loss of enzymatic activity or release of Zn^{2+} from the enzyme, showing that, once incorporated, Zn^{2+} is tightly bound and difficult to remove. Expression and purification of EaCoMT in buffers containing 1 mM EDTA, under stringent metal-free conditions, resulted in enzyme preparations containing about 0.1−0.15 Zn/monomer. It was found that this residual Zn could be removed from the enzyme upon overnight dialysis at pH 7.3 in buffer containing 5 mM CDTA, a strong zinc chelator that has been used successfully to remove Zn from the methanogenic methyltransferase MT2-A (*14*). As shown in Table 1, the apo-EaCoMT prepared in this fashion exhibited a very low specific activity and could be activated 66-fold by the addition of $ZnCl_2$. The specific activity of the Zn-reconstituted enzyme (6.6 units/mg) was approximately 60−70% of the activity of holo-EaCoMT preparations that contain, on average, 0.8−1.1 Zn/monomer. The Zn content of the Zn-reconstituted enzyme from Table 1 was analyzed by PAR/PMPS complexation and found to be 0.63 Zn/monomer.

Table 1: Activation of Zn-Deficient Apo-EaCoMT by Divalent Metal Ions[a]

divalent metal ion[b]	specific activity[c]		relative activity of apo-EaCoMT after metal ion treatment (% of holo-EaCoMT activity)
	holo-EaCoMT	apo-EaCoMT	
none	12.5 ± 0.1	0.1 ± 0.1	0.8
Zn^{2+}	9.7 ± 0.3	6.6 ± 0.01	53
Cd^{2+}	10.7 ± 0.3	4.7 ± 1.1	38
Co^{2+}	10.4 ± 0.1	2.1 ± 0.7	17
Cu^{2+}	11.4 ± 0.7	0.6 ± 0.3	4.8
Fe^{2+}	10.9 ± 0.1	2.3 ± 0.3	18
Mn^{2+}	11.9 ± 0.1	1.5 ± 0.2	12
Mg^{2+}	12.8 ± 0.1	0.2 ± 0.1	1.6
Ni^{2+}	11.1 ± 0.2	2.9 ± 0.3	23

[a] Activity assays were performed as described under Experimental Procedures using 0.0174 mg of apo-EaCoMT ([enzyme monomer] = 0.417 μM) or 0.0085 mg of holo-EaCoMT ([enzyme monomer] = 0.204 μM), 5 mM CoM, and 4 mM propylene oxide. [b] The concentration of divalent metal ion was that which gave optimal stimulation of apo-EaCoMT activity. For Co^{2+} and Cd^{2+}, the concentrations were 10 μM; for all other metal ions, the concentrations were 60 μM. [c] A unit of activity is defined as 1 μmol of propylene oxide degraded/min at 30 °C.

Grahame and co-workers have reported that reconstitution of apo-MT2-A by Zn^{2+} is stimulated by the addition of the reductant TCEP, presumably by reduction of oxidized cysteine residues that serve as ligands to the Zn^{2+} center (*14*). In our studies, we included TCEP in the Zn^{2+} reconstitution assays but were still unable to obtain preparations with increased activity or the full Zn^{2+} complement of the purified holoenzyme. The addition of the reductants dithionite or DTT did not stimulate activation or metal incorporation to any additional degree.

As shown in Table 1, other divalent metal ions, including Co^{2+}, Ni^{2+}, Fe^{2+}, and Cd^{2+}, were capable of activating apo-EaCoMT to varying degrees. This activation was specific for apo-EaCoMT: incubation of holo-EaCoMT with the same concentrations of divalent ions did not result in any stimulation of activity (Table 1). For apo-EaCoMT, the most activity after Zn^{2+} was afforded by Cd^{2+}, a highly polarizable

metal ion with high affinity for thiolates. Activation by $CoCl_2$ afforded an enzyme with 32% of the activity of the Zn-reconstituted enzyme, a result that is in agreement with previous studies of cobalt ion stimulation in Zn-deficient cell extracts (*7*). For the majority of the metal ions tested, optimal activation occurred between 10 and 60 μM M^{2+} for these incubations, which were conducted with 0.070 μM enzyme, or 0.42 μM enzyme monomer.

Stoichiometry of in Vitro M^{2+} Incorporation into Apo-EaCoMT Preparations and Stability of Apo-EaCoMT. Metal analysis of Co^{2+}-substituted, desalted enzyme preparations showed, on average, 0.4−0.6 mol of Co^{2+}/mol of enzyme monomer. Likewise, treatment of apo-EaCoMT with Zn^{2+} resulted in, on average, a maximum of 0.6−0.7 mol of tightly bound Zn^{2+}/monomer. Purified holo-EaCoMT contains, on average, 0.8−1.1 mol of Zn^{2+}/mol of monomer and ~30% higher specific activity than Zn^{2+}-activated apo-EaCoMT. Thus, it appears that not all of the potential metal binding sites in apo-EaCoMT stably incorporate metal ions during activation. This could be due to damage incurred during purification, resulting in a subset of proteins that are incapable of incorporating metal ions or which bind metal ions more weakly than holoenzyme, resulting in loss of metal upon Chelex treatment. Alternatively, some subunits of a hexameric unit may incorporate metal ions, resulting in a heterogeneous population of proteins with varying levels of M^{2+} incorporation. All attempts to stabilize apo-EaCoMT during purification, including performing enzyme preparations anaerobically and in the presence of reductants (e.g., DTT and dithionite), have failed to increase the efficiency of in vitro reconstitution.

Apo-EaCoMT appears to be inherently less stable than holo-EaCoMT on the basis of the following observations. First, prolonged incubation of the enzyme at either 4 °C or room temperature, either aerobically or anaerobically, resulted in time-dependent loss of "activatability" by divalent metal ions. At the same time, SDS−PAGE analysis revealed that apo-EaCoMT, observed as a 43 kDa band on SDS−PAGE, undergoes spontaneous cleavage to two smaller bands with apparent molecular masses of 30 and 13 kDa (data not shown). Densitometric analyses of purified apo-EaCoMT preparations showed that the 30 and 13 kDa degradation products typically accounted for 30−40% of total EaCoMT. In contrast, no detectable degradation products were seen in holo-EaCoMT preparations. The 30 and 13 kDa bands could not be separated from apo-EaCoMT by any chromatographic techniques, and apo-EaCoMT ran as a single band on an S-300 size exclusion chromatography column with the expected hexameric molecular weight of 252000. Additionally, apo-EaCoMT migrated identically to holo-EaCoMT as a single band in native PAGE gels. Thus, the observed degradation products appear to remain associated stoichiometrically within the hexameric structure of EaCoMT. The addition of protease inhibitors did not prevent this spontaneous degradation of EaCoMT in apoenzyme preparations. Thus, we conclude that the presence of the divalent metal ion is required for optimal stability of EaCoMT and that the associated ion plays a structural role as well as a catalytic role. This is evidenced in the cooperative nature of metal ion binding described below, which indicates that structural changes occur upon association of the metal ion with the six potential binding sites. Since the amount of Zn^{2+} incorporated into apo-EaCoMT directly correlates with the specific activity of the enzyme, it appears that any sites that incorporate metal ion are fully active. Thus, there is presumably heterogeneity in M^{2+}-treated apo-EaCoMT resulting from mixed populations of active high-affinity sites and inactive low-affinity sites but not due to heterogeneous metal sites with differing levels of activity.

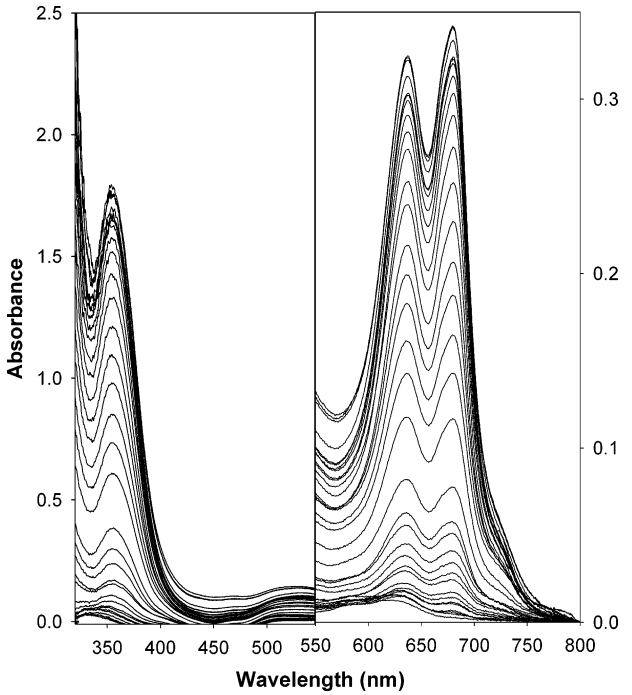

FIGURE 1: Co^{2+} reconstitution of apo-EaCoMT monitored by UV−visible spectroscopy. Each spectrum was recorded after the subsequent addition of 20 nmol (2 μL) of Co^{2+} from an anaerobically prepared stock (10 mM) to 200 μL of apo-EaCoMT (358 μM). Injections were made until an absorbance change was no longer seen (in this case, 33 injections). The absorbance scale for the d−d transitions is labeled on the right side of the figure, and the LMCT region of the spectra is labeled on the left of the figure.

Spectrophotometric Titration of Apo-EaCoMT with Co^{2+}. The Co^{2+} ion is an excellent probe for the active sites of zinc enzymes due to its similar physical properties and paramagnetism (*27*, *28*, *33*). Of potential relevance to the present work, the methanogenic CoM-dependent methytransferase MT2-A was previously prepared by Grahame and coworkers in an apo form for which reconstitution with Co^{2+} was monitored by UV−visible spectroscopy (*14*). The resultant UV−visible spectrum of the Co^{2+}-substituted enzyme suggested that Co^{2+} replaced Zn^{2+} in the same tetrahedral environment, with ligation from a combination of S and N/O ligands (*14*).

With this precedent in mind, a sample of apo-EaCoMT was prepared as described above, and the UV−visible absorption spectral changes resulting from titration with $CoCl_2$ were recorded. As shown in Figure 1, this titration resulted in the formation of three distinct peaks as well as a shoulder. Two of these peaks and a weakly visible shoulder lie within the 550−650 nm d−d charge transfer region of the spectrum. These two peaks have absorption maxima at 637 and 680 nm, and the shoulder lies at 725 nm. There is one very prominent peak in the 300−400 nm region of the spectra, which is indicative of ligand to metal charge transfer

(LMCT) from one or more metal−thiolate bond(s) (*14*, *29*, *30*, *34*). This peak has an absorption maximum at 356 nm. The protein sample was titrated with $CoCl_2$ until no further changes in absorbance were seen. At this point, the two peaks at 637 and 680 nm, in the d−d charge transfer region of the spectra, exhibited molar extinction coefficients of 1272 and 1350 M^{-1} cm^{-1}, respectively, per hexamer after correcting for enzyme dilution. The 356 nm peak seen within the LMCT region of the spectra exhibited an extinction coefficient of 7050 M^{-1} cm^{-1} per hexamer upon saturation with Co^{2+}, or 1175 M^{-1} cm^{-1} per monomer.

Upon completion of the titration showed in Figure 1, the protein sample was passed over columns of Chelex-100 and Sephadex G-25 to remove loosely bound metal ions, followed by metal analysis. This analysis showed 0.45 mol of Co^{2+}/mol of monomeric unit. When the LMCT peak (356 nm) is related to this Co^{2+} content, the extinction coefficient is 2610 M^{-1} cm^{-1}. The magnitude of LMCT bands for a single thiol−metal bond has been reported to be 900−1300 M^{-1} cm^{-1}(*34*). Thus, the magnitude of the absorption change observed upon titration of Co^{2+} into apo-EaCoMT is consistent with formation of a tetrahedral ligand environment by additional thiol ligation at the M^{2+} center, as has been proposed for other zinc alkyltransferases with the characteristic MetE−ligand binding motif (*7*, *9*). The UV−visible spectral changes observed for Co^{2+}-substituted EaCoMT are similar to, but not identical to, those observed for Co^{2+}-substituted MT2-A (*14*).

Cooperativity in Binding of Cobalt to Apo-EaCoMT. Interestingly, as can be seen in Figure 1, the first few additions of Co^{2+} led to much smaller increases in absorbance for both regions of the UV−visible spectra analyzed during the titration than for later titrations of the same amount of Co^{2+}. This result was not seen for titration of monomeric MT2-A with Co^{2+}, wherein the change in absorbance was linear up to the point of saturation (*14*). To investigate this phenomenon in more detail, the absorption of the 356 nm peak was plotted vs the total amount of Co^{2+} titrated into apo-EaCoMT. As shown in Figure 2A, a sigmoidal binding curve is seen, indicative of cooperative metal ion binding between the six binding sites in the hexameric protein. Sigmoidal curves similar to that shown in Figure 2A were also observed when either of the d−d charge transfer peaks at 637 or 680 nm was plotted on the *y*-axis.

The graph of fractional saturation vs [Co^{2+}] is presented in Figure 2B. The data points in Figure 2B were fit to the following modified form of the Hill equation (*35*):

$$f_a = pC_{TS}^{\ n}/(K_{0.5}^{\ n} + C_{TS}^{\ n}) \qquad (3)$$

where f_a is the fraction of metal sites saturated (assuming all sites are capable of binding metal), C_{TS} is the total substrate titrated, $K_{0.5}$ is the half-maximal ligand concentration, p is the proportionality factor, and n is the Hill coefficient. The solid line in Figure 2B represents the fit to eq 3, which yielded an estimated Hill coefficient of 6.1 ± 0.2. As way of comparison, a log replot of the data provided a Hill coefficient of 5.9. The plot and the Hill coefficient show that EaCoMT exhibits positive cooperativity for binding of Co^{2+}. Thus, Co^{2+} binding to the first site(s) increases the affinity of the other metal binding sites. Similar Hill coefficients were seen during steady-state reaction rates

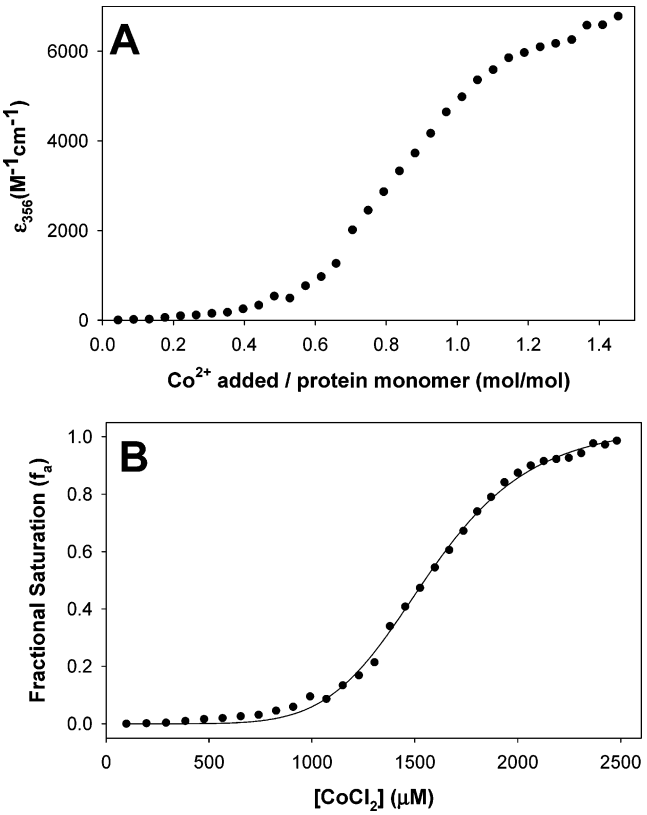

FIGURE 2: Quantification of absorbance changes resulting from Co^{2+} addition to apo-EaCoMT. Panel A: Plot of the extinction coefficient at 356 nm vs molar equivalents of Co^{2+} added (per monomeric unit, with each monomer expected to have a single metal binding site). The data were taken from the spectra shown in Figure 1 after correcting for dilution. Panel B: Plot of fractional saturation vs the concentration of Co^{2+} added. The solid line represents the fit to the modified Hill equation shown in eq 3.

in another hexameric protein, glutamate dehydrogenase (*36*). The Hill coefficients should never exceed the number of metal binding sites (*37*), which in the case of EaCoMT is six (α_6) (*3*). Thus the derived Hill coefficient from sigmoidal fit is consistent, within error, with cooperative binding to the six active sites of the hexameric enzyme.

Calorimetric Analysis of Metal Ion Binding to Apo-EaCoMT. Isothermal titration calorimetry (ITC) is a powerful technique for obtaining thermodynamic parameters for protein−ligand interactions and has been used previously to study the interaction of CoM and CoM analogues with EaCoMT (*7*). In the present study, ITC was used to investigate binding of Co^{2+} and Zn^{2+} to apo-EaCoMT in order to see whether the results of Figure 2 could be verified using an independent technique. As shown in Figures 3A and 4A, the titration of Co^{2+} or Zn^{2+} into samples of apo-EaCoMT yielded complex thermograms indicative of multiple cooperative metal binding sites (*38*−*43*). Shown in Figures 3B and 4B are the plots of the integrated heats vs amount of metal ion titrated into the enzyme, expressed as the molar ratio of metal ion to enzyme hexamer. Similar complex thermograms have been seen upon metal titration into other metal binding proteins such as carbonic anhydrase (*38*−*43*). The best fits to the data, shown in the solid lines, were obtained by using a six-site multiple-interacting binding model using the ORIGIN software provided by MicroCal. Attempts to fit the data to a multiple-interacting site model

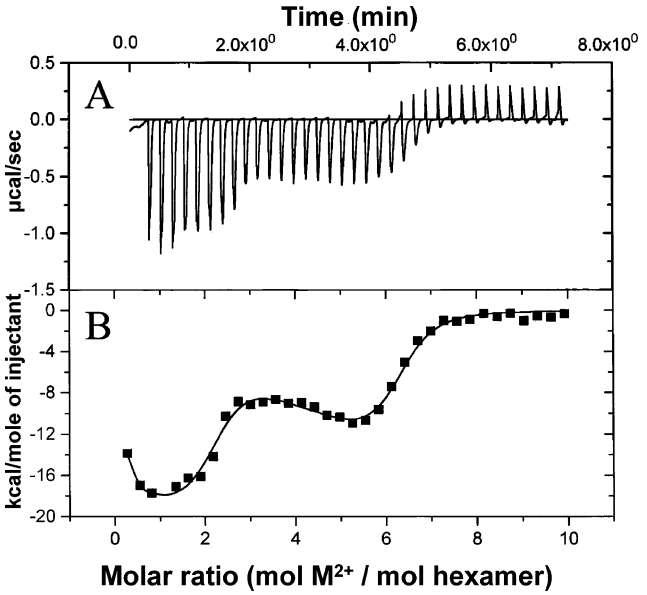

FIGURE 3: Calorimetric titration of Zn^{2+} into apo-EaCoMT. For this experiment, 10 μM EaCoMT was titrated by successive 3.5 μL injections of a 2 mM stock solution of $ZnCl_2$. Panel A shows the differential power signal recorded during the course of the experiment. Panel B shows the integrated heats plotted versus the molar ratio of ligand to protein (hexameric unit). The solid line represents the nonlinear least-squares fit of the data to a ligand binding model with six interacting sites.

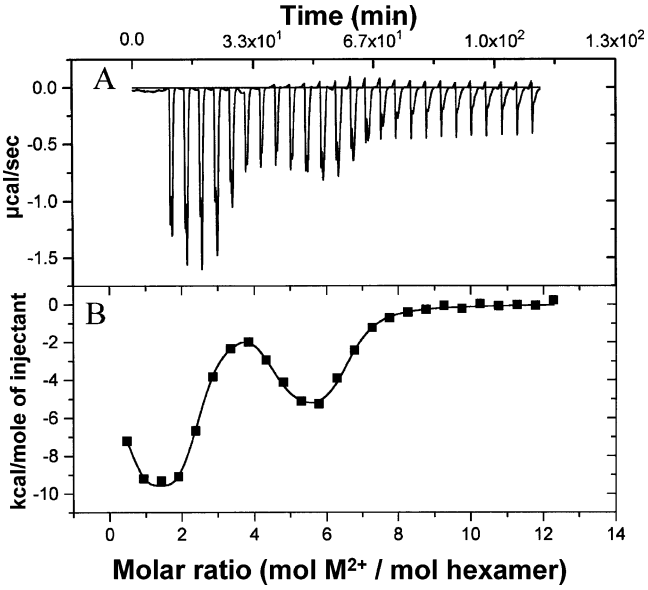

FIGURE 4: Calorimetric titration of Co^{2+} into apo-EaCoMT. For this experiment, 10 μM EaCoMT was titrated by successive 4.0 μL injections of a 1 mM stock solution of $CoCl_2$. Panel A shows the differential power signal recorded during the course of the experiment. Panel B shows the integrated heats plotted versus the molar ratio of ligand to protein (hexameric unit). The solid line represents the nonlinear least-squares fit of the data to a ligand binding model with six interacting sites.

with two, three, four, five, or seven proposed sites provided poor fits. Likewise, attempts to fit the data to a noninteracting model also failed. The average dissociation constants for the six interacting sites for the two metals were determined to be 0.61 μM for Zn^{2+} and 0.50 μM for Co^{2+}.

Formation of a New Metal−Sulfur Bond upon CoM Binding to Co^{2+}-Substituted EaCoMT. EXAFS studies of other zinc alkyltransferases, including MetE and the methanogenic methyltransferases MT2-A and MT2-M, have provided evidence that ligand exchange at the Zn center occurs upon substrate binding, with formation of a new Zn−S bond to the thiol substrate (*14*, *15*, *17*, *30*, *44*). Grahame and coworkers showed that CoM binding to Co^{2+}-substituted MT2-A resulted in UV−visible spectroscopic changes consistent with formation of a new Co^{2+}−thiol interaction (*14*). Therefore, the same methodology was applied to Co^{2+}-substituted EaCoMT to see if similar spectral changes occur upon CoM binding.

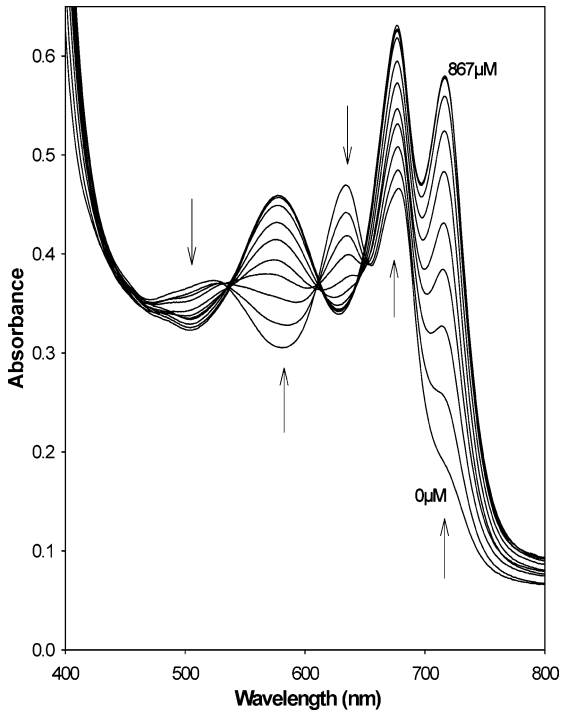

FIGURE 5: UV−visible spectroscopic analysis of CoM binding to Co^{2+}-reconstituted EaCoMT. The spectra resulting from successive 4 μL additions of CoM from a 5 mM stock solution to 304 μM Co^{2+}-EaCoMT are shown.

For this experiment, Co^{2+}-substituted EaCoMT was prepared anaerobically in the presence of excess $CoCl_2$, followed by passage over Chelex-100 and Sephadex G-25 columns to remove unbound Co^{2+}. The resultant blue protein exhibited an absorption spectrum identical to that shown for the Co^{2+}-saturated sample in Figure 1. Metal analysis of this protein sample revealed the presence of 0.42 mol of Co^{2+}/mol of protein monomer. As shown in Figure 5, titration with CoM resulted in substantial changes in the d−d transition spectral region. The most pronounced spectral changes include the transformation of the shoulder at 725 nm to a large peak at the same wavelength, an increase in the absorbance of the 677 nm peak, a decrease in the intensity of the peak seen at 637 nm, and the formation of a new peak at 577 nm. The relative magnitudes of the changes are consistent with a change in ligand environment at the metal but retention of an overall tetrahedral environment.

Within the LMCT region of the spectrum, there was a very large increase in absorbance for each CoM addition. The very large increase in absorbance in the 300−375 nm region indicates the formation of another thiol(ate) bond to the metal center upon the addition of CoM. The spectral changes associated with CoM addition to Co^{2+}-substituted EaCoMT

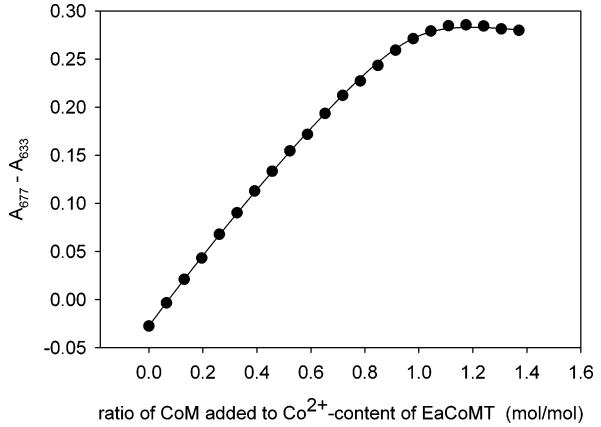

FIGURE 6: CoM binding to Co^{2+}-substituted EaCoMT. The spectral changes ($A_{677} - A_{633}$) resulting from successive 2 μL additions of CoM from a 5 mM stock solution to 304 μM Co^{2+}-EaCoMT are plotted vs the ratio of CoM to Co^{2+} content of EaCoMT. Absorbance values were corrected for dilution. The line through the data points was generated from a fit of the data to the quadratic equation as described in the text.

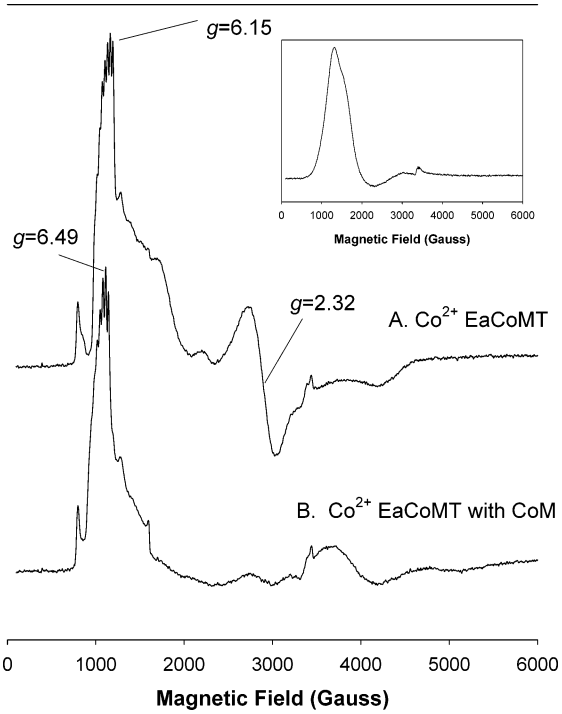

FIGURE 7: Electron paramagnetic resonance spectra of Co^{2+}-substituted EaCoMT in the absence and presence of CoM. Samples were prepared, and EPR was performed as described under Experimental Procedures. Trace A: 238 μM Co^{2+}-substituted EaCoMT. Trace B: 238 μM Co^{2+}-substituted EaCoMT with 10 mM CoM. Inset: 1.5 mM $CoCl_2$ prepared in buffer A. Experimental parameters: temperature, 5.5 K; modulation frequency, 100 kHz; modulation amplitude, 12.6 G; time constant, 81.92 ms; microwave frequency, 9.654 GHz; microwave power, 10 mW. Exact microwave frequencies were recorded in order to determine *g* values.

are consistent with retention of the overall tetrahedral environment about the metal ion but with replacement of a non-thiol ligand with the thiol of CoM.

The absorbance changes in the d−d transition region were used to quantify CoM binding to Co^{2+}-substituted EaCoMT. For this analysis, the increase in absorbance of the 677 nm peak and decrease in absorbance at 633 nm resulting from CoM addition were exploited by plotting ($A_{677} - A_{633}$) vs the concentration of CoM titrated into the enzyme sample. As shown in Figure 6, a linear increase in absorbance was observed nearly up to the saturation point. For analyzing the binding of CoM, the amount of CoM added was related to the Co^{2+} content of the enzyme sample (0.42 mol of tightly bound Co^{2+}/mol of monomer for this experiment). At the saturation point, there was an exactly 1:1 stoichiometric relationship between the amount of CoM added and the Co^{2+} content of the enzyme, supporting the idea that the divalent metal ion is crucial to thiol substrate binding (Figure 6).

For quantitative analysis of CoM binding, the data in Figure 6 were fit to the quadratic binding equation (*45*) in a manner identical to the analysis performed by Grahame and co-workers for CoM binding to Co^{2+}-substituted MT2-A (*14*). From this analysis, a K_d value for CoM of 5.37 ± 0.79 μM was derived. By comparison, the K_d for CoM binding to Zn^{2+}-EaCoMT was determined previously to be 3.8 μM by isothermal titration calorimetry (*7*). Thus, CoM binds with high affinity to both the Zn^{2+} and Co^{2+} forms of EaCoMT. As a further comparison, Co^{2+}-substituted MT2-A was shown by the same technique to bind CoM with K_d = 7.0 μM (*14*). Thus, the Co^{2+} forms of both enzymes behave similarly with respect to CoM binding and affinity. Importantly, no cooperativity for CoM binding was observed for either Zn^{2+}- (*7*) or Co^{2+}-EaCoMT (Figure 6). Likewise, kinetic studies have shown that both epoxypropane and CoM interact with EaCoMT according to normal Michaelis−Menten kinetics (*7*). Thus, while EaCoMT exhibits cooperativity for metal ion binding to the apoenzyme, once the metals are bound, there is no cooperativity with regard to substrate binding on the six active sites in the hexameric enzyme.

EPR Characterization of Cobalt-Substituted EaCoMT. The EPR spectra of Co^{2+}-substituted EaCoMT were recorded in the absence and presence of CoM in order to gain additional insights into the metal−thiolate interactions. Cobalt ion was chosen as a probe of the active site of EaCoMT because the ion complexes are extremely sensitive to coordination environment (*46*). As shown in Figure 7, Co^{2+}-substituted EaCoMT exhibited a complex EPR spectrum that was perturbed upon addition of CoM. The spectrum in the absence of CoM is indicative of a high-spin $S = {}^3/_2$ Co^{2+} center and has features similar to those observed for tetrahedrally coordinated Co^{2+}-substituted enzymes (*27*, *47*−*53*), some of which coordinate metal ion with sulfur ligands (*51*, *54*−*57*). The upfield component at $g = 6.15$ (1178 G) is relatively narrow and exhibits $I = {}^7/_2$ nuclear hyperfine splitting due to the ^{59}Co nucleus, with a hyperfine coupling constant of $A = 33$ G. This eight-line hyperfine splitting is slightly off center on the low-field absorption feature (g_{max}), indicating that there may be more than one signal-giving species in the spectrum (*47*). There are also other fine structure details in the spectrum. These include peaks at $g = 4.33$ (1589 G), $g = 3.21$ (2152 G), and $g = 1.85$ (3729 G) as well as a rhombic signal centered at $g = 2.32$ (2975 G). There is also a peak at $g = 1.92$ (3583 G) which may have a nonresolvable Co^{2+} $I = {}^5/_2$ nuclear hyperfine structure. Similar upfield hyperfine splitting around $g = 2$ has been seen in model complexes (*58*). This spectrum implies that the metal binding site has low symmetry

(E/D > 0) and the cobalt ion is highly constrained. The number of ligands about the cobalt ion cannot be determined from the hyperfine splitting or the observed *g*-values because six-, five-, or four-coordinate geometries show spectral similarities (*46*, *47*).

Upon addition of CoM to the enzyme, large perturbations in the EPR spectrum are seen (Figure 7B). A large narrow signal can be seen at $g = 6.49$ with distinct ^{59}Co hyperfine splitting and an *A* value of 30 G, indicating that the metal is still enzyme bound and in the high-spin Co^{2+} $S = {}^3/_2$ state. There are also accessory peaks at $g = 4.33$ (1594 G), $g = 2.53$ (2726 G), and $g = 1.88$ (3718 G). Additionally, the rhombic $g = 2.32$ peak and valley seen in the Co^{2+}-EaCoMT is nearly absent in the CoM + Co^{2+}-EaCoMT spectrum. Numerous differences can be noted in the two spectra, most notably the downfield shift of the g_{max} peak containing nuclear hyperfine splitting, and the rhombic signal at $g = 2.32$ is diminished in the sample with CoM. These differences indicate that the addition of CoM changes the electronic geometry of the metal from a relatively rhombic geometry to a more axial geometry.

Included in Figure 7, as an inset, is a spectrum of 1.5 mM $CoCl_2$ taken under the same conditions as the Co^{2+}-EaCoMT and CoM + Co^{2+}-EaCoMT spectra. The large, broad, g_{max} signal is centered at $g = 5.2$ (1330 G), or upfield from the g_{max} signal in the protein spectra, and lacks the nuclear hyperfine splitting. The small inflections at $g \sim 2$ in all three spectra are caused by a Cu^{2+} contamination in the cavity of the EPR spectrophotometer. The addition of CoM to the 1.5 mM solution of $CoCl_2$ did not result in any significant changes in the EPR spectrum (data not shown).

Deprotonation of CoM by Zn^{2+}- and Cd^{2+}-Substituted EaCoMT. By analogy to other zinc alkyltransferases, metal ion coordination of CoM in EaCoMT is believed to lower the pK_a of the thiol to generate the requisite thiolate for attack on the second substrate epoxypropane (*7*, *11*, *15*, *18*, *22*, *29*, *44*). For other zinc alkyltransferases, proton release from the thiol substrate has been demonstrated directly by spectrophotometrically monitoring the change in absorbance of the pH-dependent dye phenol red upon titration of the thiol substrate into a solution of the enzyme (*8*, *59*). To determine whether proton release could be observed similarly for EaCoMT, CoM was titrated into solutions of apoEaCoMT and apoEaCoMT reconstituted with Zn^{2+}, Co^{2+}, or Cd^{2+}, and the resultant change in absorbance of phenol red at 558 nm was used to quantify the extent of substrate deprotonation.

Very little proton release from CoM was observed in samples of apoEaCoMT. However, as shown in Figure 8, each of the divalent metal ion-reconstituted enzymes stimulated proton exchange in an apparently saturable fashion. For quantitative analysis, proton release from CoM was related to the metal ion contents of the three reconstituted enzyme samples (Figure 8). The data were fit to a rectangular hyperbola using the equation:

$$H = H_{max}[\mathrm{CoM}]/(K_{d(obs)} + [\mathrm{CoM}]) \qquad (4)$$

where *H* is the moles of H^+ released per mole of enzyme monomer and H_{max} is the theoretical maximal number of protons released per mole of enzyme monomer. The hyperbolic fits provided the following kinetic parameters: Zn^{2+}-substituted enzyme, $K_d = 16.5 \pm 0.83$ μM and $H_{max} = 0.94 \pm 0.02$ mol of H^+/mol of Zn^{2+}; Co^{2+}-substituted enzyme, $K_d = 13.1 \pm 0.59$ μM and $H_{max} = 0.89 \pm 0.02$ mol of H^+/mol of Co^{2+}; Cd^{2+}-substituted enzyme, $K_d = 12.0 \pm 0.47$ μM and $H_{max} = 1.1 \pm 0.02$ mol of H^+/mol of Cd^{2+}. Thus, there is a largely 1:1 stoichiometric relationship between stimulation of proton release from CoM and metal ion content, supporting the idea that coordination of CoM to the metal ion may be responsible for lowering the pK_a of the thiol. The K_d values observed are all in the same range and largely in agreement with the K_d values obtained for CoM binding to Zn-containing (holo) EaCoMT by ITC [3.8 μM (*7*)] and Co^{2+}-substituted EaCoMT by spectroscopic titration (5.37 μM, Figure 6).

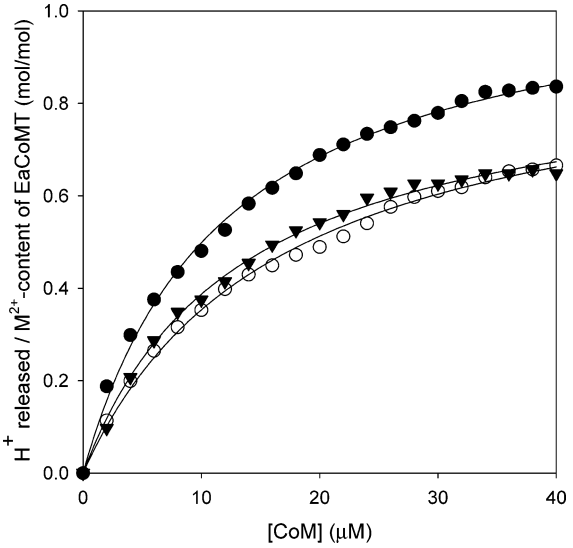

FIGURE 8: Proton release by apo-EaCoMT and metal-substituted EaCoMT. Assays involving change in absorbance of phenol red were performed as described under Experimental Procedures. Absorbance values were recorded after 2 μL additions of a 1 mM CoM stock solution. Data are plotted as mol of H^+ released/mol of metal ion bound to the enzyme. The concentrations of enzyme were 30 μM (monomer concentration) in all assays. Metal contents of the desalted and dialyzed proteins are indicated below. The lines through the data points represent the fits to a rectangular hyperbola (eq 4). Symbols: (▼) Co^{2+}-substituted EaCoMT (0.60 mol of Co^{2+}/mol of monomer); (○) Zn^{2+}-substituted EaCoMT (0.58 mol of Zn^{2+}/mol of monomer); (●) Cd^{2+}-substituted EaCoMT (0.62 mol of Cd^{2+}/mol of monomer).

DISCUSSION

This paper provides the first direct spectroscopic evidence for the role of the zinc ion site of EaCoMT in CoM binding and activation for nucleophilic attack on the second substrate epoxypropane. To accomplish this, an inactive, zinc-deficient form of EaCoMT was prepared and subsequently activated with Co^{2+}, an excellent paramagnetic probe for the active sites of Zn^{2+} enzymes (*28*). The magnitude of the absorption change observed upon complete titration of Co^{2+} into apo-EaCoMT (Figure 1), when correlated with the Co^{2+} content of the reconstituted enzyme, is consistent with formation of a tetrahedral ligand environment with two thiolate ligands at the newly formed Co^{2+} center (Figure 1) (*14*, *28*). The UV−visible and EPR spectral changes that are observed upon CoM addition to Co^{2+}-substituted EaCoMT show that the environment of the Co^{2+} center is altered dramatically upon CoM binding to the enzyme (Figures 5 and 7). The most straightforward explanation for these spectral changes

is that the thiol of CoM directly ligates the Co^{2+} center, either by displacing an exchangeable ligand or by increasing the coordination number about Co^{2+}.

EXAFS studies of other zinc alkytransferases with the characteristic "MetE" metal binding motif support the idea of ligand exchange upon thiol substrate binding (*14*, *15*, *18*, *60*, *61*). In the case of MetE, EXAFS studies indicated that the substrate-free enzyme contained Zn^{2+} in a tetrahedral environment with 2S and 2 N/O atoms ligated to Zn^{2+} (*9*, *18*, *61*). The addition of homocysteine resulted in the loss of one N/O ligand and its replacement by an additional S, with retention of the tetrahedral environment (*9*, *18*, *61*). Evidence for ligand exchange involving replacement of a N/O atom by S has also been obtained from EXAFS studies of the methanogenic CoM methyltransferases MT2-A and MT2-M (*14*, *15*).

Recently, the three-dimensional structures of MetE enzymes from two different organisms, *Arabidopsis thaliana* and *Thermotoga maritima*, have been solved by X-ray crystallography, both in the presence and in the absence of the substrate homocysteine (*19*, *20*). For the *A. thaliana* MetE, Zn^{2+} in the resting enzyme was coordinated to His647, Cys649, and Cys733, the proposed permanent ligands, as well as an exogenous water ligand, in a tetrahedral environment. Unexpectedly, the structure of the homocysteine-bound enzyme did not show the ligand exchange predicted from EXAFS analyses; instead, there was a reorganization of the Zn^{2+} center, with stronger coordination of the two permanent thiol ligands Cys649 and Cys733 and the exogenous water molecule, with no change in coordination of His647 (*19*). The distance from the sulfur of homocysteine to Zn^{2+} was between 3.6 and 4.4 Å, indicating no direct interaction of the thiol with Zn^{2+} (*19*). For the *T. maratima* MetE, some notable differences were observed. First, the resting enzyme contained a Glu residue (Glu642) bound to the Zn^{2+} center in place of the water observed as the fourth ligand in *A. thaliana* MetE (*20*). Second, the addition of homocysteine resulted in a change in coordination geometry about Zn^{2+} from tetrahedral to distorted trigonal bipyramidal, with the S of homocysteine and O of Glu642 assuming the axial positions (*20*). The Zn−S and Zn−O bond distances observed for these axial ligands were unusually long (2.9−3.15 Å) for such a complex.

At present, it is unclear why the two MetE structures exhibit different environments for the Zn^{2+} center, both in the substrate-free and in the homocysteine-bound forms. It is also unclear how these studies relate to the extensive spectroscopic studies of MetE and homologues, which in all cases suggest ligand exchange at the Zn^{2+} center upon thiol substrate binding. The structure of *A. thaliana* MetE was obtained at pH 6.5, while that of *T. maratima* MetE was obtained at pH 5.2. Perhaps the differences in pH account for some of the structural differences observed. Spectroscopic studies of MetE were performed at higher pH values (7 and above) than those used for crystallography; this difference in pH may account for differences in how homocysteine ligates the Zn^{2+} center. In any event, the crystal structures introduce the potential for debate on the role of the Zn^{2+} center of MetE and homologues, i.e., whether direct coordination or another mechanism is responsible for lowering the pK_a of the thiol substrate. The UV−visible and EPR spectroscopic results presented here for Co^{2+}-substituted EaCoMT support a model where CoM directly coordinates the metal ion, but it is conceivable that the spectral changes could result from other ligand rearrangements resulting from CoM binding.

Of the alkyltransferases with a "MetE Zn^{2+} binding motif" that have been studied with regard to metal ion binding and activation, EaCoMT is unique in having a hexameric structure. The hexameric nature of EaCoMT and the apparent cooperativity for metal ion binding add a new level of complexity for this enzyme. The calorimetric and UV−visible titration studies show that EaCoMT binds metal ions cooperatively at six dependent sites. However, upon desalting and chelation, only about 50% of the expected metal ions are retained. These results suggest that the apo-EaCoMT preparations used for these experiments have both high-affinity and low-affinity metal binding sites, possibly due to damage incurred during purification as mentioned in the Results section. Importantly, the results in this paper show that the metal ions that are retained with high affinity (i.e., after chelator treatment and desalting) are catalytically active and capable of coordinating CoM, as evidenced by the 1:1 stoichiometry between Co^{2+} content and CoM bound (Figures 5 and 6). It is not certain whether the high-affinity sites are distributed among mixed populations of hexameric units with varying metal contents or a population of fully loaded hexamers along with a population of inactive metal-free hexamers.

In summary, the results of the present work demonstrate the importance of a divalent metal ion in CoM activation and deprotonation by EaCoMT and provide spectroscopic evidence for a metal ion−CoM interaction. While it is possible that the bound metal ion plays a structural role rather than a catalytic one, the evidence presented herein favors a direct catalytic role for the metal ion through the intermediacy of a metal−thiolate bond. The results provide a foundation for further biochemical, spectroscopic, and structural studies to characterize the metal center and catalytic mechanism of this unique alkyltransferase.

ACKNOWLEDGMENT

We are grateful to Dr. John Peters for helpful discussions.

REFERENCES

1. Small, F. J., and Ensign, S. A. (1997) Alkene monooxygenase from *Xanthobacter* strain Py2: Purification and characterization of a four-component system central to the bacterial metabolism of aliphatic alkenes, *J. Biol. Chem. 272*, 24913−24920.
2. Ensign, S. A. (2001) Microbial metabolism of aliphatic alkenes, *Biochemistry 40*, 5845−5853.
3. Allen, J. R., and Ensign, S. A. (1997) Purification to homogeneity and reconstitution of the individual components of the epoxide carboxylase multiprotein enzyme complex from *Xanthobacter* strain Py2, *J. Biol. Chem. 272*, 32121−32128.
4. Allen, J. R., Clark, D. D., Krum, J. G., and Ensign, S. A. (1999) A role for coenzyme M (2-mercaptoethansulfonic acid) in a bacterial pathway of aliphatic epoxide carboxylation, *Proc. Natl. Acad. Sci. U.S.A. 96*, 8432−8437.
5. Ensign, S. A., and Allen, J. R. (2003) Aliphatic epoxide carboxylation, *Annu. Rev. Biochem. 72*, 55−76.
6. Coleman, N. V., and Spain, J. C. (2003) Distribution of the coenzyme M pathway of epoxide metabolism among ethene- and vinyl chloride-degrading *Mycobacterium* strains, *Appl. Environ. Microbiol. 69*, 6041−6046.
7. Krum, J. G., Ellsworth, H., Sargeant, R. R., Rich, G., and Ensign, S. A. (2002) Kinetic and microcalorimetric analysis of substrate

and cofactor interactions in epoxyalkane:CoM transferase, a zinc-dependent epoxidase, *Biochemistry 41*, 5005−5014.
8. Goulding, C. W., and Matthews, R. G. (1997) Cobalamin-dependent methionine synthase from *Escherichia coli*: Involvement of zinc in homocysteine activation, *Biochemistry 36*, 15749−15757.
9. Zhou, Z. H. S., Peariso, K., Penner-Hahn, J. E., and Matthews, R. G. (1999) Identification of the zinc ligands in cobalamin-independent methionine synthase (MetE) from *Escherichia coli*, *Biochemistry 38*, 15915−15926.
10. Myers, L. C., Verdine, G. L., and Wagner, G. (1993) Solution structure of the DNA methyl phosphotriester repair domain of *Escherichia coli* Ada, *Biochemistry 32*, 14089−14094.
11. Saderholm, M. J., Hightower, K. E., and Fierke, C. A. (2000) Role of metals in the reaction catalyzed by protein farnesyltransferase, *Biochemistry 39*, 12398−12405.
12. Breksa, A. P., and Garrow, T. A. (1999) Recombinant human liver betaine-homocysteine S-methyltransferase: Identification of three cysteine residues critical for zinc binding, *Biochemistry 38*, 13991−13998.
13. Thanbichler, M., Neuhierl, B., and Bock, A. (1999) S-methylmethionine metabolism in *Escherichia coli*, *J. Bacteriol. 181*, 662−665.
14. Gencic, S., LeClerc, G. M., Gorlatova, N., Peariso, K., Penner-Hahn, J. E., and Grahame, D. A. (2001) Zinc-thiolate intermediate in catalysis of methyl group transfer in *Methanosarcina barkeri*, *Biochemistry 40*, 13068−13078.
15. Krüer, M., Haumann, M., Meyer-Klaucke, W., Thauer, R. K., and Dau, H. (2002) The role of zinc in the methylation of the coenzyme M thiol group in methanol:coenzyme M methyltransferase from *Methanosarcina barkeri*, *Eur. J. Biochem. 269*, 2117−2123.
16. Krum, J. G., and Ensign, S. A. (2000) Heterologous expression of bacterial epoxyalkane:coenzyme M transferase and inducible coenzyme M biosynthesis in *Xanthobacter* strain Py2 and *Rhodococcus* rhodochrous B276, *J. Bacteriol. 182*, 2629−2634.
17. González, J. C., Peariso, K., Penner-Hahn, J. E., and Matthews, R. G. (1996) Cobalamin-independent methionine synthase from *Escherichia coli:* A zinc metalloenzyme, *Biochemistry 35*, 12228−12234.
18. Peariso, K., Zhou, Z. H. S., Smith, A. E., Matthews, R. G., and Penner-Hahn, J. E. (2001) Characterization of the zinc sites in cobalamin-independent and cobalamin-dependent methionine synthase using zinc and selenium X-ray absorption spectroscopy, *Biochemistry 40*, 987−993.
19. Ferrer, J. L., Ravanel, S., Robert, M., and Dumas, R. (2004) Crystal structure of cobalamin-independent methionine synthase complexed with zinc, homocysteine, and methyltetrahydrofolate, *J. Biol. Chem. 279*, 44235−44238.
20. Pejchal, R., and Ludwig, M. L. (2005) Cobalamin-independent methionine synthase (MetE): A face-to-face double barrel that evolved by gene duplication, *PLOS Biol. 3*, 254−265.
21. Matthews, R. G., and Goulding, C. W. (1997) Enzyme-catalyzed methyl transfers to thiols: the role of zinc, *Curr. Opin. Chem. Biol. 1*, 332−339.
22. Sauer, K., and Thauer, R. K. (2000) Methyl-coenzyme M formation in methanogenic archaea−Involvement of zinc in coenzyme M activation, *Eur. J. Biochem. 267*, 2498−2504.
23. Tallant, T. C., Paul, L., and Krzycki, J. A. (2001) The MtsA subunit of the methylthiol:coenzyme M methyltransferase of *Methanosarcina barkeri* catalyses both half-reactions of corrinoid-dependent dimethyl sulfide:coenzyme M methyl transfer, *J. Biol. Chem. 276*, 4485−4493.
24. Taylor, C. D., and Wolfe, R. S. (1974) Structure and methylation of coenzyme M ($HSCH_2CH_2SO_3$), *J. Biol. Chem. 249*, 4879−4885.
25. Wolfe, R. S. (1991) My kind of biology, *Annu. Rev. Microbiol. 45*, 1−35.
26. Thauer, R. K. (1998) Biochemistry of methanogenesis: a tribute to Marjory Stephenson, *Microbiology 144*, 2377−2406.
27. Bertini, I., Luchinat, C., and Viezzoli, M. S. (1986) in *Zinc Enzymes* (Bertini, I., Luchinat, C., Maret, W., and Zeppezauer, M., Eds.) pp 24−27, Birkhouser, Boston, MA.
28. Maret, W., and Vallee, B. (1993) Cobalt as a probe and label of proteins, *Methods Enzymol. 226*, 52−71.
29. Hightower, K. E., Huang, C. C., Casey, P. J., and Fierke, C. A. (1998) H−Ras peptide and protein substrates bind protein farnesyltransferase as an ionized thiolate, *Biochemistry 37*, 15555−15562.
30. Huang, C.-C., Casey, P. J., and Fierke, C. A. (1997) Evidence for a catalytic role for zinc in protein farnesyltransferase: Spectroscopy of Co^{2+}-farnesyltransferase indicates metal coordination of the substrate thiolate, *J. Biol. Chem. 272*, 20−23.
31. Alberty, R. A. (1996) IUPAC-IUBMB Joint Commission on Biochemical Nomenclature (JCBN). Recommendations for nomenclature and tables in biochemical thermodynamics, *Eur. J. Biochem. 240*, 1−14.
32. Chromy, V., Fischer, J., and Kulhanek, V. (1974) Re-evaluation of EDTA-chelated biuret reagent, *Clin. Chem. 20*, 1362−1363.
33. Bertini, I., Luchinat, C., and Monnanni, R. (1985) Zinc Enzymes, *J. Chem. Educ. 62*, 924−927.
34. May, S. W., and Kuo, J. (1978) Preparation and properties of cobalt(II) rubredoxin, *Biochemistry 17*, 3333−3338.
35. Creighton, T. E. (1993) *Proteins: Structure and Molecular Properties*, 2nd ed., W. H. Freeman, New York.
36. Wang, X. G., and Engel, P. C. (1995) Positive cooperativity with Hill coefficients of up to 6 in the glutamate concentration dependence of steady-state reaction rates measured with clostridial glutamate dehydrogenase and the mutant A163G at high pH, *Biochemistry 34*, 11417−11422.
37. Frank, P., Angove, H. C., Burgess, B. K., and Hodgson, K. O. (2001) Determination of ligand binding constants for the iron−molybdenum cofactor of nitrogenase: monomers, multimers, and cooperative behavior, *J. Biol. Inorg. Chem. 6*, 683−697.
38. DiTusa, C. A., Christensen, T., McCall, K. A., Fierke, C. A., and Toone, E. J. (2001) Thermodynamics of metal ion binding. 1. Metal ion binding by wild-type carbonic anhydrase, *Biochemistry 40*, 5338−5344.
39. Gopal, B., Swaminathan, C. P., Bhattacharya, S., Bhattacharya, A., Murthy, M. R. N., and Surolia, A. (1997) Thermodynamics of metal ion binding and denaturation of a calcium binding protein from *Entamoeba histolytica*, *Biochemistry 36*, 10910−10916.
40. DiTusa, C. A., McCall, K. A., Christensen, T., Mahapatro, M., Fierke, C. A., and Toone, E. J. (2001) Thermodynamics of metal ion binding. 2. Metal ion binding by carbonic anhydrase variants, *Biochemistry 40*, 5345−5351.
41. Patel, D. R., Jao, C. C., Mailliard, W. S., Isas, J. M., Langen, R., and Haigler, H. T. (2001) Calcium-dependent binding of annexin 12 to phopholipid bilayers: Stoichiometry and implications, *Biochemistry 40*, 7054−4060.
42. Henzl, M. T., Hapak, R. C., and Likos, J. J. (1998) Interconversion of the ligand arrays in the CD and EF sites of oncomodulin. Influence of Ca^{2+}-binding affinity, *Biochemistry 37*, 9101−9111.
43. Barney, B. M., LoBrutto, R., and Francisco, W. A. (2004) Characterization of a small metal binding protein from *Nitrosomonas europaea*, *Biochemistry 43*, 11206−11213.
44. Myers, L. C., Terranova, M. P., Ferentz, A. E., Wagner, G., and Verdine, G. L. (1993) Repair of DNA methylphosphotriesters through a metalloactivated cysteine nucleophile, *Science 261*, 1164−1167.
45. Segel, I. H. (1975) *Enzyme Kinetics*, John Wiley and Sons, New York.
46. Adrait, A., Jacquamet, L., Le Pape, L., Gonzalez de Peredo, A., Aberdam, D., Hazemann, J., Latour, J., and Michaud-Soret, I. (1999) Spectroscopic and saturation magnetization properties of the manganese- and cobalt-substituted Fur (ferric uptake regulation) protein from *Escherichia coli*, *Biochemistry 38*, 6248−6260.
47. Bennett, B., and Holz, R. C. (1997) Spectroscopically distinct cobalt(II) sites in heterodimetallic forms of the aminopeptidase from *Aeromonas proteolytica*: Characterization of substrate binding, *Biochemistry 36*, 9837−9846.
48. Shapir, N., Osborne, J. P., Johnson, G., Sadowsky, M. J., and Wackett, L. P. (2002) Purification, Substrate range, and metal center of AtzC: The N-isopropylammelide aminohydrolase involved in bacteral atrazine metabolism, *J. Bacteriol. 184*, 5376−5384.
49. Sytkowski, A. J., and Vallee, B. (1978) Cobalt exchange in horse liver alcohol dehydrogenase, *Biochemistry 17*, 2850−2857.
50. D'souza, V. M., Bennett, B., Copik, A. J., and Holz, R. C. (2000) Divalent metal binding properties of the methionyl aminopeptidase from *Escherichia coli*, *Biochemistry 39*, 3817−3826.
51. Gavel, O. Y., Bursakov, S. A., Calvete, J. J., George, G. N., Moura, J. J., and Moura, I. (1998) ATP sulfurylases from sulfate-reducing bacteria of the genus *Desulfovibrio.* A novel metalloprotein containing cobalt and zinc, *Biochemistry 37*, 16225−16232.
52. Martinelli, R. A., Hanson, G. R., Thompson, J. S., Holmquist, B., Pilbrow, J. R., Auld, D. S., and Vallee, B. (1989) Characterization

of the Inhibitor complexes of cobalt carboxypeptidase A by electron paramagnetic resonance spectroscopy, *Biochemistry 28*, 2251−2258.
53. Bubacco, L., Magliozzo, R. S., Beltramini, M., Salvato, B., and Peisach, J. (1992) Preparation and spectroscopic characterization of a coupled binuclear center in cobalt(II)-substituted hemocyanin, *Biochemistry 31*, 9294−9303.
54. Good, M., and Vasak, M. (1986) Spectroscopic properties of the cobalt(II)-substituted a-fragment of rabbit liver metallothionein, *Biochemistry 25*, 3328−3334.
55. Makinen, M. W., and Yim, M. (1981) Coordination environment of the active-site metal ion of liver alcohol dehydrogenase, *Proc. Natl. Acad. Sci. U.S.A. 78*, 6221−6225.
56. Dworschack, R. T., and Plapp, B. V. (1977) pH, isotope, and substituent effects on the interconversion of aromatic substrates catalyzed by hydroxybutyrimidylated liver alcohol dehydrogenase, *Biochemistry 16*, 2716−2725.
57. Moura, I., Teixeira, M., LeGall, J., and Moura, J. J. (1991) Spectroscopic studies of cobalt and nickel substituted rubredoxin and desulforedoxin, *J. Inorg. Biochem. 44*, 127−139.
58. Horrocks, W., Ishley, J. N., Holmquist, B., and Thompson, J. S. (1980) Structural and electronic mimics of the active site cobalt-(II)-substituted zinc metalloenzymes, *J. Inorg. Biochem. 12*, 131−141.
59. Sauer, K., and Thauer, R. K. (1999) Methanol:coenzyme M methyltransferase from *Methanosarcina barkeri*—substitution of the corrinoid harbouring subunit MtaC by free cob(I)alamin, *Eur. J. Biochem. 261*, 674−681.
60. Peariso, K., Zhou, Z. H. S., Smith, A. E., Huang, S., Matthews, R. G., and Penner-Hahn, J. E. (1999) Characterization of the zinc binding site in cobalamin-independent and cobalamin-dependent methionine synthase from *Escherichia coli* via X-ray absorption spectroscopy, *J. Inorg. Biochem. 74*, 262−262.
61. Peariso, K., Goulding, C. W., Huang, S., Matthews, R. G., and Penner-Hahn, J. E. (1998) Characterization of the zinc binding site in methionine synthase enzymes of *Escherichia coli:* The role of zinc in the methylation of homocysteine, *J. Am. Chem. Soc. 120*, 8410−8416.

BI0505619